

# A Study of effect of tip mass density, orientation and resistance on vibration energy harvester

Laxmi.B.Wali<sup>1\*</sup>, C V Chandrasekhara<sup>2</sup>

<sup>1</sup>Assistant Professor, Department of Mechanical Engineering, RNSIT, VTU, Bengaluru, Karnataka, INDIA

<sup>2</sup>Professor, Design Lead, Department of Mechanical Engineering, PES University, Bengaluru, Karnataka, INDIA

## Abstract:

Energy harvesting is extracting energy from ambient sources. Vibration energy harvesting area have received attention of many researchers to power wireless sensors and low-power electronic devices from smart materials. In this paper, effect of tip mass density, orientation and resistance on cantilever beam bounded with piezoelectric patch is studied. The analytical equations of beam is derived using Euler Bernoulli beam assumptions, constitutive equations of piezoelectric material and Hamilton's principle.

**Keywords:** Orientation, Energy harvesting, Vibration, piezoelectric, FEM, Orientation.

**DOI:** [10.24297/j.cims.2023.2.8](https://doi.org/10.24297/j.cims.2023.2.8)

---

## 1. Introduction

Energy harvesting is scavenging energy from sources available in the surrounding environment [1]. Vibration energy is one of the source available freely from machines, human motion having low frequency excitation which can be used to meet the demand without depending on conventional sources. Restriction in battery capacity to power the devices and life span for supplying continuous energy for wireless technologies necessitate for energy harvesting. Piezoelectric materials are currently generating a demand and forms the alternate source for the creation of lifelong energy harvesters with compact configuration which will be utilized in various applications. Research of piezoelectric elements in energy conversion applications necessitates a thorough understanding of solid mechanics and geometrical shapes [2]. Researchers have focused on analytical and numerical studies of unimorph and bimorph beam which forms the basis for the study of energy harvesting due to its compatibility and ease of application [3-6]. Study on orientation of harvester for rotational motion by changing the distance between the rotating centre and fixed end of beam on one end and tip mass on free end [7] and study on configurations of energy harvester for IoT sensor applications in smart

cities [8] is carried by researchers and Comparison of unimorph and bimorph beam with tip mass is studied and authors concluded that, increase in tip mass increases voltage [9]. Researchers focused on simulation in COMSOL Multiphysics for beam without considering the effect of tip mass [10] Study on optimal location of piezoelectric patch on the length of slat in aircraft applications is studied [11, 12] and piezoelectric harvesters are considered to give higher output compared to electrostatic and electromagnetic energy harvesters and device size has to be optimized to get maximum output [13]. A less information is available in the literature on the study of orientation of the beam with tip mass on free end and base excitation at fixed end. The aim of this work is to obtain output by developing the MatLab program for the study of orientation of unimorph cantilever beam with tip mass, to get voltage, current and power frequency response function and describe its dynamic behaviour by varying tip mass density, orientation of beam and resistance for first, second and third natural frequencies.

## 2. Methodology

The Finite element method plays the major role in the complex problem analysis. In vibration based energy harvesting, piezoelectric unimorph beam forms the basic structure. The formulation of beam with piezoelectric (PZT) layer is considered as shown in Fig.1

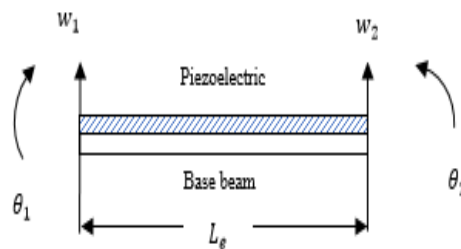


Figure 1 .Element with base beam bounded with PZT

The beam with piezoelectric has two degree of freedom at each node, transverse ( $w$ ) and rotational ( $\theta$ )

The displacement function of the beam element is given as

$$w(x) = c_0 + c_1x + c_2x^2 + c_3x^3 \quad (1)$$

Eqn. 1 is the displacement equation with four unknown coefficients. Applying boundary conditions at node 1 and 2 of element, the four coefficients in polynomial equation are solved.

The shape functions are given in equation (2-5)

$$[N] = [N_1 \quad N_2 \quad N_3 \quad N_4]$$

where

$$[N_1] = \left( 1 - 3 \left( \frac{x}{L_e} \right)^2 + 2 \left( \frac{x}{L_e} \right)^3 \right) \quad (2)$$

$$[N_2] = \left( L_e \left( x - 2 \left( \frac{x}{L_e} \right)^2 + \left( \frac{x}{L_e} \right)^3 \right) \right) \quad (3)$$

$$[N_3] = \left( 3 \left( \frac{x}{L_e} \right)^2 - 2 \left( \frac{x}{L_e} \right)^3 \right) \quad (4)$$

$$[N_4] = \left( L_e \left( - \left( \frac{x}{L_e} \right)^2 + \left( \frac{x}{L_e} \right)^3 \right) \right) \quad (5)$$

Strain  $S(x)$  is represented by

$$S(x) = -z \frac{d^2 w(x)}{dx^2} = -zB \quad (6)$$

Where  $B = [B_1, B_2, B_3, B_4]$

Differentiating Eq. (2-5)

$$\frac{d^2 N_1}{dx^2} = \frac{-6}{L_e^2} + \frac{12x}{L_e^3} = B_1 \quad (7)$$

$$\frac{d^2 N_2}{dx^2} = \frac{-4}{L_e} + \frac{6x}{L_e^2} = B_2 \quad (8)$$

$$\frac{d^2 N_3}{dx^2} = \frac{6}{L_e^2} - \frac{12x}{L_e^3} = B_3 \quad (9)$$

$$\frac{d^2 N_4}{dx^2} = \frac{-2}{L_e} + \frac{6x}{L_e^2} = B_4 \quad (10)$$

The electromechanical coupling of a piezoelectric can be demonstrated in two ways. In direct piezoelectric effect, an applied mechanical pressure produces a proportional voltage response and in converse effect, an applied voltage produces a deformation of the material.

The direct effect and the converse effect may be modelled as

$$\{D\} = [e]^T \{S\} + [\varepsilon^S] \{E\} \quad (11)$$

$$\{T\} = [c^E] \{S\} - [e] \{E\} \quad (12)$$

The constitutive equation for 1-dimensional form with constant electric field and strain is

$$\begin{Bmatrix} T_1 \\ D_3 \end{Bmatrix} = \begin{bmatrix} c_{11}^E & -e_{31} \\ e_{31} & \varepsilon_{33}^S \end{bmatrix} \begin{Bmatrix} S_1 \\ E_3 \end{Bmatrix} \quad (13)$$

The base beam and piezoelectric plane stress field equation is given by Eq.14 and 15

$$T_1^{(1)} = c_{11}^{(1)} S_1^{(1)} \quad (14)$$

$$T_1^{(2)} = c_{11}^{(2)} S_1^{(2)} - e_{31} E_3 \quad (15)$$

$\vartheta(z) = \frac{z-z_n+h_p}{h_p}$  is the shape function over the interval  $z_n - h_p \leq z \leq z_n$

$z_n = \frac{c_{11}^{(1)}h_s^2 + c_{11}^{(2)}h_p^2 + 2c_{11}^{(1)}h_s h_p}{2(c_{11}^{(1)}h_s + c_{11}^{(2)}h_p)}$  = distance from the neutral axis to the top layer of the beam with piezoelectric

$\varphi(z) = \vartheta(z)v_p$  is electrical potential

$\Omega(z)$  = first derivative of shape function =  $\frac{d\vartheta(z)}{dz} = 1/h_p$ ,

The electric field equation

$$E_3 = -\Omega(z)v_p \quad (16)$$

where  $v_p$  = voltage

Substituting Equation (6) into Equation (14)

$$T_1^{(1)} = -zc_{11}^{(1)}B \quad (17)$$

Substituting Equation (6) and (16) into Equation (15)

$$T_1^{(2)} = -zc_{11}^{(2)}B + e_{31}\Omega(z)v_p(t) \quad (18)$$

$$D_3 = -ze_{31}B - \varepsilon_{33}^S \Omega(z)v_p \quad (19)$$

The electromechanical piezoelectric cantilever energy harvesting is formulated by the Hamiltonian principle,

$$\int_{t_1}^{t_2} [\delta(k - \dot{p} + \omega) + \delta\varpi] dt = 0 \quad (20)$$

Representation of equations in matrix form utilizing extended Hamilton' s principle [3]

$$\begin{bmatrix} M & 0 \\ 0 & 0 \end{bmatrix} \begin{Bmatrix} \dot{w} \\ \dot{v}_p \end{Bmatrix} + \begin{bmatrix} C & 0 \\ P_{sr} & P_D \end{bmatrix} \begin{Bmatrix} \dot{w} \\ \dot{v}_p \end{Bmatrix} + \begin{bmatrix} K & P_{rs} \\ 0 & 0 \end{bmatrix} \begin{Bmatrix} w \\ v_p \end{Bmatrix} = \begin{Bmatrix} F \\ i_p \end{Bmatrix} \quad (21)$$

Element Stiffness Eq.22, mass matrix Eq.23 is given by

$$[K] = \int z^2 c_{11}^{(1)} [B^T] [B] dv^{(1)} + \int z^2 c_{11}^{(2)} [B^T] [B] dv^{(2)} \quad (22)$$

$$[M] = \int \rho^{(1)} [N^T] [N] dv^{(1)} + \int \rho^{(2)} [N^T] [N] dv^{(2)} \quad (23)$$

Adding tip mass terms to Eq. (23)

$$2I_0^{tip} x_c [N^T] \frac{d[N]}{dx} + I_0^{tip} [N^T] [N] + I_2^{tip} \frac{d[N^T]}{dx} \frac{d[N]}{dx} \quad (24)$$

Offset distance from proof mass centroid [5] is

$$x_c = \frac{\rho^{tip} b l_{tip}^2 h_{tip} + \rho^{(1)} b l_{tip}^2 h_s}{2(\rho^{tip} b l_{tip} h_{tip} + \rho^{(1)} b l_{tip} h_s)} \quad (25)$$

Zeroth and second mass moment of inertia [5] is given by

$$I_0^{tip} = \rho^{tip} b l_{tip} h_{tip} + \rho^{(1)} b l_{tip} h_s \quad (26)$$

$$\begin{aligned} I_2^{tip} = & \left( \rho^{tip} b l_{tip} h_{tip} \left( \frac{l_{tip}^2 + h_{tip}^2}{12} \right) + \rho^{tip} b l_{tip} h_{tip} \left( z_n - h_p + \frac{h_{tip}}{2} \right)^2 + \left( \frac{l_{tip}}{2} \right)^2 \right) \\ & + \left( \rho^{(1)} b l_{tip} h_s \left( \frac{l_{tip}^2 + h_s^2}{12} \right) \right. \\ & \left. + \rho^{(1)} b l_{tip} h_s \left( -z_n - h_p + \frac{h_s}{2} \right)^2 \left( \frac{l_{tip}}{2} \right)^2 \right) \end{aligned} \quad (27)$$

Damping matrix C is given as

$$C = \alpha M + \beta K \quad (28)$$

Mechanical Force F is given by

$$F = -Q \ddot{w}_{base} \quad (29)$$

Where

$$Q = \int \rho^{(1)} N^T dV^{(1)} + \int \rho^{(2)} N^T dV^{(2)} \quad (30)$$

Adding tip mass terms to Eq. (29)

$$-I_0^{tip} x_c \frac{d[N^T]}{dx} - I_0^{tip} [N^T] \quad (31)$$

Electromechanical coupling is given by

$$P_{sr} = - \int z \Omega(z)^T e_{31} B dV^{(2)} \quad (32)$$

Capacitance matrix is given by

$$P_D = - \int \Omega(z)^T \epsilon_{33} \Omega(z) dV^{(2)} \quad (33)$$

Transformation matrix is given by

$$T = [\cos(\theta) \ 0 \ 0 \ 0; \ 0 \ 1 \ 0 \ 0; \ 0 \ 0 \ \cos(\theta) \ 0; \ 0 \ 0 \ 0 \ 1]$$

Formulating the Eq. (21).into global matrix based on electromechanical vector transformation.

Voltage, current and power frequency response function obtained by direct non-

orthonormalised electromechanical dynamic equation is given by [4]

$$\frac{v_p}{-\omega w_b e^{j\omega t}} = \left[ j\omega C_p - \frac{1}{R_{load}} j\omega \theta^T * [\underline{K} - \omega^2 \underline{M} + j\omega \underline{C}]^{-1} \theta \right]^{-1} * j\omega \theta^T [\underline{K} - \omega^2 \underline{M} + j\omega \underline{C}]^{-1} Q \quad (34)$$

$$\frac{i}{-\omega^2 w_{base} e^{i\omega t}} = \frac{1}{R_{load}} \left\{ [C_p i\omega + R_l - \theta^T i\omega [-\underline{M}\omega^2 + \underline{C}i\omega + \underline{K}]^{-1} \theta]^{-1} * \theta^T i\omega [-\underline{M}\omega^2 + \underline{C}i\omega + \underline{K}]^{-1} Q \right\} \quad (35)$$

$$\frac{P}{(-\omega^2 w_{base} e^{i\omega t})^2} = \frac{1}{R_{load}} \left\{ [C_p i\omega + R_l - \theta^T i\omega [-\underline{M}\omega^2 + \underline{C}i\omega + \underline{K}]^{-1} \theta]^{-1} * \theta^T i\omega [-\underline{M}\omega^2 + \underline{C}i\omega + \underline{K}]^{-1} Q \right\}^2 \quad (36)$$

The dynamic equations are solved assuming system response is linear under harmonic base excitation and beam is excited in transverse direction. The electromechanical piezoelectric cantilever energy harvesting beam equations are formulated by the Hamiltonian principle.

**Table 1** Geometry and material properties

Length, $l$	50e-3 (m)	Modulus of Elasticity of the PZT, $E_p$	66 (Gpa)
Width, $b$	6e-3 (m)	Density, $\rho^{(1)}$	9000 (kg/m <sup>3</sup> )
Thickness, $h_b$	0.5e-3 (m)	Density of the PZT layer, $\rho^{(2)}$	7800 (kg/m <sup>3</sup> )
Thickness of PZT, $h_p$	0.190e-3 (m)	Piezoelectric constant, $e_{31}$	-12.54 (C/m <sup>2</sup> )
Modulus of Elasticity of the base beam, $E_b$	105 (Gpa)	Permittivity of constant strain, $\epsilon_{p33}$	1.3555 e-008
Length of tip mass	15 (mm)	height of tip mass	10 (mm)
Density of tip mass	9000 (kg/m <sup>3</sup> )	Damping constant	$\alpha=4.88$ 6; $\beta=1.24$ 33e-05

The numerical work of the author [4] is extended to outline the key equations and include the tip mass and orientation for the electromechanical dynamic equation.

### 3. Results and Discussion

#### 3.1 Model of orientated beam bounded with piezoelectric patches and tip mass

The study on energy harvesting is carried on cantilever beam of length 'L'. The beam is divided into two parts  $L/2$  each.

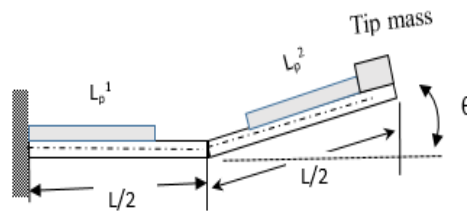


Figure 2 Orientation of Cantilever beam bounded with piezoelectric patches and tip mass at free end.

The geometrical and material property of the beam are presented in table 1. Tip mass is mounted on extended length of base beam. The length of the piezoelectric patches  $L_{p1}$  and  $L_{p2}$  is 20 mm each. The angle of orientations ' $\theta$ ' of the beam is  $10^\circ$ ,  $30^\circ$  and  $50^\circ$ . The analysis of the beam is carried out using MATLAB program in the frequency range of 0 to 1000 Hz. The Cantilever beam of length 'L' is divided into 50 elements

Orientation of beam in degrees	First 3 natural frequencies for tip mass density in $\text{kg/m}^3$		
	7800	8000	8200
10	24.22	23.94	23.67
	210.30	208.18	206.13
	909.90	908.59	907.33
20	23.60	23.33	23.06
	212.07	209.92	207.83
	906.05	904.80	903.61
30	22.52	22.25	22.00
	214.97	212.75	210.61
	899.49	898.36	897.29

Table 2 shows that, as the tip mass density increases first, second and third natural frequency decreases. As the orientation of beam increases, first and third natural frequency decreases with increase in second natural frequency.

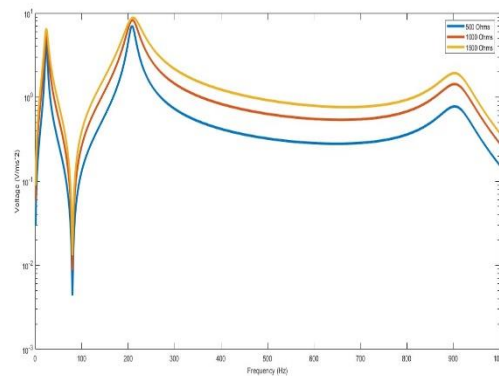


Figure 3 Voltage FRF of  $10^0$  orientation of beam and tip mass density of  $8000\text{kg/m}^3$

Figure 3 shows the voltage frequency response function for the beam oriented at  $10^0$  orientation and tip mass density of  $8000\text{kg/m}^3$  for resistance of  $500\Omega$ ,  $1000\Omega$  and  $1500\Omega$ . From the graph it is seen that, as the resistance increases voltage increases for first, second and third natural frequencies.

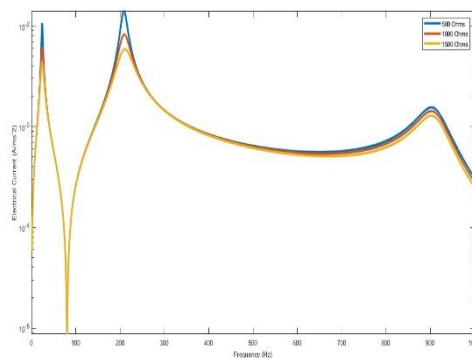


Figure 4 Current FRF of  $10^0$  orientation of beam and tip mass density of  $8000\text{kg/m}^3$

Figure 4 shows the current frequency response function for the beam oriented at  $10^0$  orientation and tip mass density of  $8000\text{kg/m}^3$  for resistance of  $500\Omega$ ,  $1000\Omega$  and  $1500\Omega$ . From the graph it is seen that, as the resistance increases current decreases for first, second and third natural frequencies.

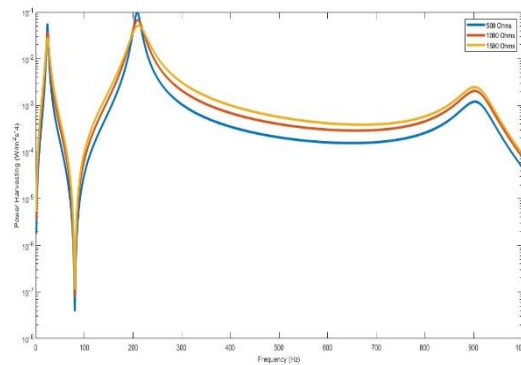


Figure 5 Power FRF of  $10^{\circ}$  orientation of beam and tip mass density of  $8000\text{kg/m}^3$

Figure 5 shows the power frequency response function for the beam oriented at  $10^{\circ}$  orientation and tip mass density of  $8000\text{kg/m}^3$  for resistance of  $500\Omega$ ,  $1000\Omega$  and  $1500\Omega$ . From the graph it is seen that, as the resistance increases power decreases for first, second frequency and increases for third natural frequency.

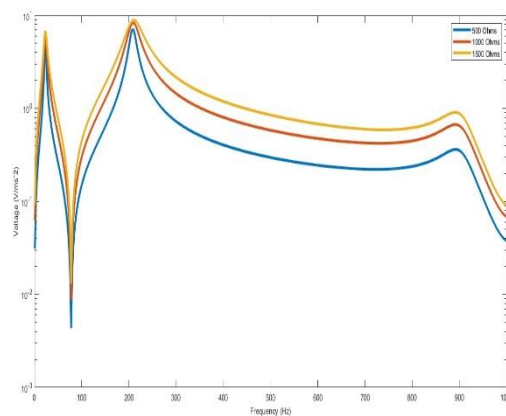


Figure 6 Voltage FRF for  $20^{\circ}$  orientation of beam and tip mass density of  $8200\text{kg/m}^3$

Figure 6 shows the voltage frequency response function for the beam oriented at  $20^{\circ}$  orientation and tip mass density of  $8200\text{kg/m}^3$  for resistance of  $500\Omega$ ,  $1000\Omega$  and  $1500\Omega$ . From the graph it is seen that, as the resistance increases voltage increases for first, second and third natural frequencies.

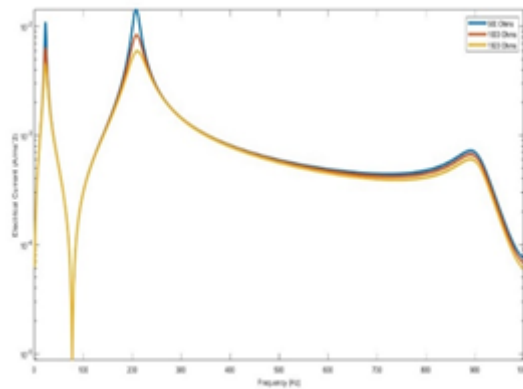


Figure 7 Current FRF for  $20^{\circ}$  orientation of beam and tip mass density of  $8200\text{kg/m}^3$

Figure 7 shows the current frequency response function for the beam oriented at  $20^{\circ}$  orientation and tip mass density of  $8200\text{kg/m}^3$  for resistance of  $500\Omega$ ,  $1000\Omega$  and  $1500\Omega$ . From the graph it is seen that, as the resistance increases current decreases for first, second and third natural frequencies.

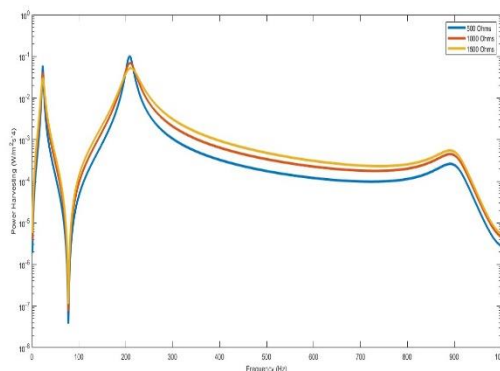


Figure 8 Power FRF for  $20^{\circ}$  orientation of beam and tip mass density of  $8200\text{kg/m}^3$

Figure 8 shows the power frequency response function for the beam oriented at  $20^{\circ}$  orientation and tip mass density of  $8200\text{kg/m}^3$  for resistance of  $500\Omega$ ,  $1000\Omega$  and  $1500\Omega$ . From the graph it is seen that, as the resistance increases power decreases for first, second frequency and increases for third natural frequency

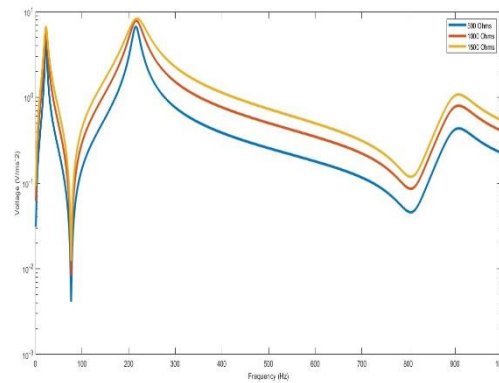


Figure 9 Voltage FRF of  $30^{\circ}$  orientation of beam and tip mass density of  $7800 \text{ kg/m}^3$

Figure 9 shows the voltage frequency response function for the beam oriented at  $30^{\circ}$  orientation and tip mass density of  $7800 \text{ kg/m}^3$  for resistance of  $500 \Omega$ ,  $1000 \Omega$  and  $1500 \Omega$ . From the graph it is seen that, as the resistance increases voltage increases for first, second and third natural frequencies.

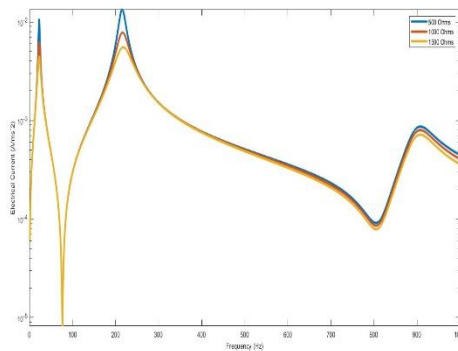


Figure 10 Current FRF of  $30^{\circ}$  orientation of beam and tip mass density of  $7800 \text{ kg/m}^3$

Figure 10 shows the current frequency response function for the beam oriented at  $30^{\circ}$  orientation and tip mass density of  $7800 \text{ kg/m}^3$  for resistance of  $500 \Omega$ ,  $1000 \Omega$  and  $1500 \Omega$ . From the graph it is seen that, as the resistance increases current decreases for first, second and third natural frequencies.

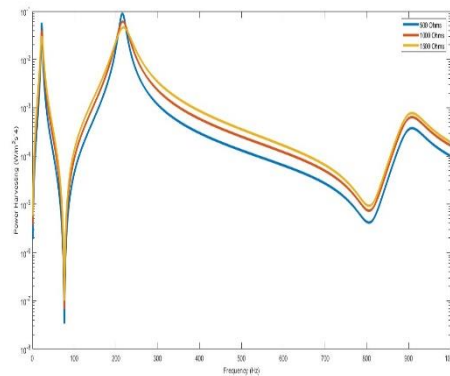


Figure 11 Power FRF of  $30^{\circ}$  orientation of beam and tip mass density of  $7800 \text{ kg/m}^3$

Figure 11 shows the power frequency response function for the beam oriented at  $30^{\circ}$  orientation and tip mass density of  $7800 \text{ kg/m}^3$  for resistance of  $500 \Omega$ ,  $1000 \Omega$  and  $1500 \Omega$ . From the graph it is seen that, as the resistance increases power decreases for first, second frequency and increases for third natural frequency.

Figures 3-11 shows the voltage, current and power FRF for  $10^{\circ}$ ,  $20^{\circ}$ ,  $30^{\circ}$  orientation of beam and tip mass density of  $8000$ ,  $8200$  and  $7800 \text{ kg/m}^3$ . From the observations, it is concluded that as

As density of tip mass increases, 3 natural frequencies decreases with increase in voltage, current and power.

As resistance increases, voltage increases and current decreases for first, second and third natural frequencies. Power decreases for first and second natural frequencies and increases for third natural frequency.

As the angle of orientation of beam increases from  $10^{\circ}$  to  $30^{\circ}$ , voltage, current and power increases.

## References

1. Shad Roundy, Paul K. Wright, Jan Rabaey, A study of low level vibrations as a power source for wireless sensor nodes, Computer Communications 2003.
2. Henry A. Sodano and Daniel J. Inman ,A Review of Power Harvesting from Vibration using Piezoelectric Materials, The Shock and Vibration Digest. 2004; 36(3), 197-205.

3. A.Erturk, D. J. Inman, A Distributed Parameter Electromechanical Model for Cantilevered Piezoelectric Energy Harvesters, *Journal of Vibration and Acoustics* 2008
4. Eziwarman, Mikail F. Lumentut, Comparative Numerical Studies of Electromechanical Finite Element Vibration Power Harvester Approaches of a Piezoelectric Unimorph. *IEEE/ASME International Conference on Advanced Intelligent Mechatronics (AIM)* Besançon, France 201
5. Usama H. Hegazy ,Nonlinear Dynamics of a Controlled Cantilever Beam with Varying Orientation under Primary Resonance, *American Journal of Mechanical Engineering*, 2014, Vol. 2, No. 7, 316-327
6. Mikail F.Lumentut, Ian M.Howard Parametric design-based modal damped vibrational piezoelectric energy harvesters with arbitrary proof mass offset: Numerical and analytical validations, *Mechanical Systems and Signal Processing* 2016, 68-69 562–586
7. Wei-Jiun Su et.al, Analysis of a Cantilevered Piezoelectric Energy Harvester in Different Orientations for Rotational Motion, *Sensors* 2020 MDPI
8. Iman Izadgoshasb, Piezoelectric Energy Harvesting towards Self-Powered Internet of Things (IoT) Sensors in Smart Cities, *Sensors* 2021 MDPI
9. Yunbin Chen, Zhi Yan, Nonlinear analysis of unimorph and bimorph piezoelectric energy harvesters with flex electricity, *Composite Structures*, 2021
10. Indrajit Chandra Das and et.al, Design, Simulation & Optimization of a MEMS Based Piezoelectric Energy Harvester, *International Journal of Scientific & Engineering Research* Volume 12, Issue 7, July-2021
11. Jiang Ding et.al, A piezoelectric energy harvester using an arc-shaped piezoelectric cantilever beam array, *Microsystem Technologies* 2022
12. Domenico Tommasino et.al, Vibration Energy Harvesting by Means of Piezoelectric Patches: Application to Aircrafts, *Sensors* 2022 MDPI
13. Weipeng Zhou, Recent Research Progress in Piezoelectric Vibration Energy Harvesting Technology, *Energies* 2022, MDPI